

## Rapid communication

# High temperature oxidation of Cr–N coatings prepared by high power pulsed magnetron sputtering – Plasma immersion ion implantation & deposition



Zhongzhen Wu <sup>a, b</sup>, Xiubo Tian <sup>b, \*\*</sup>, Shu Xiao <sup>a</sup>, Chunzhi Gong <sup>b</sup>, Feng Pan <sup>a, \*</sup>, Paul K. Chu <sup>c</sup>

<sup>a</sup> School of Advanced Materials, Peking University Shenzhen Graduate School, Shenzhen 518055, China

<sup>b</sup> State Key Laboratory of Advanced Welding Production and Technology, Harbin Institute of Technology, Harbin 150001, China

<sup>c</sup> Department of Physics and Materials Science, City University of Hong Kong, Tat Chee Avenue, Kowloon, Hong Kong, China

## ARTICLE INFO

## Article history:

Received 29 April 2014

Received in revised form

11 May 2014

Accepted 2 June 2014

Available online 14 June 2014

## Keywords:

HPPMS-PIII&D

Cr–N

High temperature oxidation

Corrosion resistance

## ABSTRACT

Good oxidation and corrosion resistance are required for cutting tools and other industrial components used in high temperature applications. The highest operational temperature of CrN is normally about 500 °C. A denser Cr–N coating prepared by high power pulsed magnetron sputtering – plasma immersion ion implantation & deposition shows oxidation resistance up to 800 °C compare with those prepared by conventional magnetron sputtering. The hardness and corrosion resistance are shown and discussed. The enhanced performance can be attributed to a phase transition from CrN to Cr<sub>2</sub>N during annealing and there is no obvious oxide formation on the coatings.

© 2014 Elsevier Ltd. All rights reserved.

Good thermal oxidation resistance and corrosion resistance are needed for high-speed cutting tools and industrial components used in harsh environments, for instance, pipelines, boilers, etc. [1–3] and a feasible method to protect the components from high temperature oxidation and corrosion is to apply a surface coatings. However, there are normally oxidation and corrosion channels in coatings prepared by conventional PVD methods such as cathodic arc deposition and magnetron sputtering because cavities induced by the “macro-particles” and low energetic deposition, respectively [4,5].

High power pulsed magnetron sputtering – plasma immersion ion implantation & deposition (HPPMS-PIII&D) is a relatively new hybrid technology [6,7] combining high plasma ionization of high power pulsed magnetron sputtering (HPPMS) and consequent high energetic ion acceleration of plasma immersion ion implantation & deposition (PIII&D). By combining the high ionization efficiency in HPPMS and energetic ion bombardment and implantation rendered by PIII&D, an extra dense coatings with better oxidation

and corrosion resistance can be prepared [8,9]. CrN is commonly applied as a coating due to its excellent oxidation and corrosion resistance but CrN coatings prepared by conventional PVD methods resist oxidation and degradation of mechanical properties only up to about 500 °C [10,11] which is insufficient in many demanding applications.

In this work, Cr–N coatings are prepared by HPPMS-PIII&D and the oxidation and corrosion resistance of the Cr–N coatings is studied after annealing at different temperatures. The performance of these coatings is compared to that produced by conventional direct-current magnetron sputtering (DCMS) and high power pulsed magnetron sputtering (HPPMS) with –100 V DC bias. The Cr–N coatings prepared by the HPPMS-PIII&D deliver outstanding protection even after the annealing at a temperature as high as 800 °C.

Deposition was performed in a vacuum chamber (40 cm in diameter and 80 cm in height) evacuated by a turbo-molecular pump and it was carried out in three stages. Firstly, a Cr layer was produced on Si (100) (for SEM and TEM observation) and SU201 stainless steel (for other tests) substrates by HPPMS-PIII&D at 780 V, 50 Hz and 200 μs in an inert atmosphere. The high-voltage pulses applied to the substrates had amplitudes of –8 kV, –12 kV, –16 kV, and –20 kV and the same frequency and width as those of the HPPMS pulses. The high voltage and HPPMS

\* Corresponding author. Tel./fax: +86 755 26033200.

\*\* Corresponding author. Tel./fax: +86 451 86418784.

E-mail addresses: [wuzhongzhen2003@163.com](mailto:wuzhongzhen2003@163.com) (Z. Wu), [xiubotian@163.com](mailto:xiubotian@163.com) (X. Tian), [panfeng@pkusz.edu.cn](mailto:panfeng@pkusz.edu.cn) (F. Pan).

pulses were synchronized by a matching circuit [6]. The working pressure was kept 1.0 Pa for 5 min. The substrates were placed at a distance of 16 cm from the target and not treated during deposition. In the second stage,  $N_2$  was introduced into the vacuum chamber gradually until the flow rate ratio of Ar to  $N_2$  was 5:3. Cr–N thin films with a thickness of 1.5  $\mu\text{m}$  were deposited in this mixed atmosphere. Finally, cool down in the vacuum chamber for 30 min. For comparison, conventional DCMS and HPPMS were conducted to deposit Cr–N at a DC bias of  $-100$  V and the same power as that in HPPMS-PIII&D. The thickness and Cr/N ratio of the materials prepared by DCMS and HPPMS are similar to those prepared by HPPMS-PIII&D at  $-12$  kV, which is about 1:1.

After deposition, the samples were annealed in an oven for 1 h at  $200$   $^{\circ}\text{C}$ ,  $400$   $^{\circ}\text{C}$ ,  $600$   $^{\circ}\text{C}$ , or  $800$   $^{\circ}\text{C}$ . The microstructure and thickness of the coatings were evaluated by scanning electron microscopy (SEM) on a 30 kV Hitachi S4800 instrument. The cross sections and interfaces were examined by high-resolution transmission electron microscopy (FE-TEM, FEI-TECNAIG2-F30, USA). X-ray diffraction (XRD) was performed to investigate the phase composition of the films using the Bragg–Brentano geometry. A Cu  $K_{\alpha}$  radiation source was used (40 kV, 40 mA). An MTS nano-indenter XP2 equipped with a Berkovich diamond indenter was used to measure the hardness and Young's modulus of the samples and the corrosion behaviors of the samples were studied by electrochemical methods. A computer-assisted electrochemical apparatus was used to obtain the potential–current curves. The polarization plots were acquired in a 3.5% NaCl solution at a scanning rate of 5 mV/s.

Fig. 1 depicts the SEM cross-sectional micrographs of the Cr–N films fabricated by DCMS and HPPMS with DC bias of  $-100$  V and HPPMS-PIII&D with pulsed bias of  $-12$  kV. The DCMS sample exhibits a loosely packed columnar structure (Fig. 1a) and most of columnar grains are continuous from the substrate to the coating surface. A columnar structure typically forms during low-energy deposition due to low adatom mobility [12]. A well-defined boundary and abrupt interface appear between the substrate and Cr–N film indicative of potentially bad film adhesion. The HPPMS sample shows a dense granular nano-crystalline structure and clean interface are observed [13]. In comparison, the HPPMS-PIII&D

sample shows a most densely packed columnar structure (Fig. 1b) and most of the columns are discontinuous. The top columns seem to form on the broken columns quickly due to re-nucleation [14]. An extra dense structure without any cavities can be observed between the Cr–N columnar crystals (Fig. 1c). The interface provides a direct contact between the dense granular nano-crystalline Cr interlayer and substrate thus promoting the formation of metallic, covalent, or ionic bonds as opposed to the significantly weaker van der Waals bonds (Fig. 1d). Formation of the dense coating and compact interface arises from the relatively high energy of about 12 keV and consequent thermal diffusion [15].

Fig. 2 displays the XRD spectra acquired from the as-prepared Cr–N films fabricated by DCMS and HPPMS at a DC bias of  $-100$  V and HPPMS-PIII&D at pulsed biases of  $-8$  kV,  $-12$  kV,  $-16$  kV, and  $-20$  kV. For the DCMS and HPPMS samples, the CrN(200), Cr<sub>2</sub>N(113) peak and some peaks stemming from the substrate can be observed. The intensity of the peaks is low and some peaks are broad suggesting the existence of amorphous or nano-crystals in the films. A large difference can be observed from the HPPMS-PIII&D samples which show a highly preferential orientation of CrN(200) and some weaker peaks introduced by the stainless steel substrate. With increasing pulsed biases, the intensity of the CrN(200) peak decreases and the Cr<sub>2</sub>N(111) peak appears when the pulsed bias is larger than  $-16$  kV. The phase evolution may depend on the N contents in the Cr–N coatings which decrease because more Cr ions are attracted to the substrate while the Ar/N ratio in the ambient is kept constant.

Fig. 3 shows the XRD spectra of the Cr–N films fabricated by DCMS and HPPMS at  $-100$  V and HPPMS-PIII&D at  $-12$  kV after annealing at different temperature from room temperature to  $800$   $^{\circ}\text{C}$ . When the annealing temperature is below  $600$   $^{\circ}\text{C}$ , there are nearly no peak changes in all the Cr–N coatings. prepared by DCMS and HPPMS. However, many new peaks such as CrN(110), Cr<sub>2</sub>N(302), Cr<sub>2</sub>N(111), Cr<sub>2</sub>N(221), Cr<sub>2</sub>O<sub>3</sub>(104), Cr<sub>2</sub>O<sub>3</sub>(300), and Cr<sub>2</sub>O<sub>3</sub>(210) emerge on the Cr–N coatings prepared by DCMS and HPPMS after annealing at  $600$   $^{\circ}\text{C}$  and they increase further after annealing at  $800$   $^{\circ}\text{C}$  (Fig. 3a). The peak intensity of the DCMS sample increases with annealing temperature, indicating continuous oxidation and also re-crystallization [16]. The oxidation of the

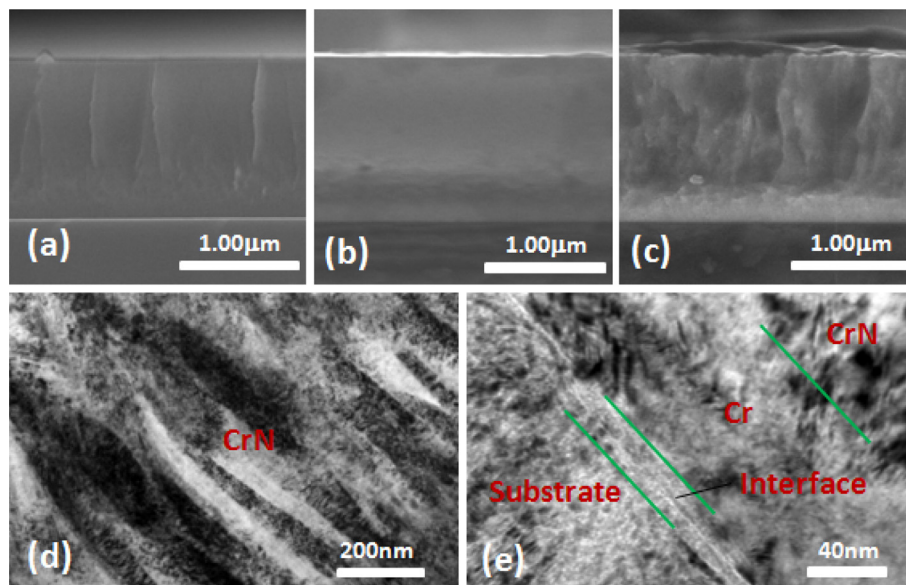


Fig. 1. Cross-sectional SEM morphology of the Cr–N coatings fabricated by (a) DCMS at  $-100$  V DC bias, (b) HPPMS at  $-100$  V DC bias and (c) HPPMS-PIII&D at  $-12$  kV pulsed bias; (d) Cross-sectional TEM morphology of Cr–N columns in the HPPMS-PIII&D sample and (e) Interface between the Cr–N coating and substrate of the HPPMS-PIII&D sample.

Download English Version:

<https://daneshyari.com/en/article/1689860>

Download Persian Version:

<https://daneshyari.com/article/1689860>

[Daneshyari.com](https://daneshyari.com)